High Temperature Pile Irradiation of the *n*-Heptane-Hydrogen System

GEORGE H. MILEY and JOSEPH J. MARTIN

University of Michigan, Ann Arbor, Michigan

A pilot unit for the high-temperature irradiation of flowing reactants was designed for the beam port of a nuclear reactor. Radiation-thermal cracking of the *n*-heptane-hydrogen system was studied with molal H_2/C_7 ratios from 0 to 5 at 250 lb./sq. in., 600° to 750°F., 2 to 8 min. residence time, and up to 3,600 rep./min. Although conversions were low, the decomposition rate was significantly increased by radiation giving G values $> 10^3$. Product distributions were not significantly altered by radiation. These results, while different from low-temperature data, appear consistent with other published high-temperature results. Radiation yields were found to be reasonably linear with total dose from 0 to 14 krep., but a twofold increase was observed in passing from a molal H_2/C_7 ratio of 0 to 0.5.

Although the radiation decomposition of organic compounds has been studied extensively, a majority of these studies have been concerned with room-temperature effects and have utilized cobalt-60 or machine radiation sources (*1, 2*). The possibility of using a full scale nuclear reactor to produce process steam and simultaneously irradiate chemicals has led to experiments with reactor radiation and elevated temperatures (*3* to *8*). Lucchesi et al. (*7*) reported a study of the high temperature radio-cracking (radiation decomposition) of several organic systems with *G* values far larger than those reported for low-temperature irradiations. The present work was designed to extend these studies to the *n*-heptane-hydrogen system.

APPARATUS

Irradiations were carried out in the University of Michigan's Ford Nuclear Reactor, a 1-mw. swimming pool type (*9, 10, 11*). Two beam ports, designated G and J, were utilized. Experiments in J port used a fission plate (an encased uranium slab placed against the end of the port to increase the fast neutron flux).

A flow-system pilot unit was designed to handle multistream, liquid-gas, chemical reactions at high temperature and pressure (Figure 1). External equipment such as the feed pumping and product separation section are fairly conventional and are described elsewhere (*9*). The irradiation vessel involved unique problems (Figure 2). The unusual shape is a result of space limitations imposed by the beam port. Reactants enter the lower section and flow under the horizontal baffle plate to the end of the vessel nearest the nuclear reactor core before exiting. A calrod heater was immersed in the lower half of the vessel, and the vessel and inlet lines were wrapped with heating tape and asbestos insulation. Thermocouples were located on the vessel shell, on inlet and outlet lines, and at 3-in. intervals in the thermowell. A cooling coil provided an additional means of temperature regulation. Type 304 stainless steel was used throughout. Because induced radioactivity made direct maintenance impossible after initial exposure, special precautions were taken to prevent plugging. A strainer was placed at the vessel outlet, and the inlet line was recessed to permit cleaning with a reverse gas purge.

The irradiation vessel was attached to the end of a shielding plug made of a 5 ft. x 8 in. diameter aluminum pipe filled with barytes concrete. Several sections of ¾-in. tubing in 360-deg. spirals were embedded in the concrete to permit passage of utility lines without radiation streaming.

In addition to requirements for personnel safety the possibility of damage to the nuclear reactor presented a serious problem. Extreme safety factors were used, and extensive testing was done prior to insertion in the beam port.

EXPERIMENTAL PROCEDURE AND SAMPLE ANALYSIS

Over seventy runs were made with the *n*-heptane-hydrogen system covering the range of variables shown in Table 1. Pressure and local temperature variations of less than ± 10 lb./sq.in. and ± 5°F. were obtained. Each radiation run was paired with a blank made with the nuclear reactor shut down. The reactor had a fresh fuel loading so background gamma activity from fission product build-up was inherently low. Shutdown periods of 24 hr. or more were allowed prior to blank runs, and the entire series was run within a month after insertion to minimize induced radioactivity in vessel walls. Both calculations and actual dosimetry measurements showed that under these conditions decomposition due to background radiation could be neglected.

Liquid samples were analyzed with partition chromatography with trimetacresyl phosphate on fire brick at 120°C. with helium gas carrier. The C_7 cut was examined for unsaturation with infrared techniques. Gas samples were analyzed with a mass spectrometer.

Complete liquid and gas samples were taken during initial runs. Data showed that liquid phase conversion (the mole percent cracked hydrocarbons in the liquid product as measured by chromatography) could be correlated with the total *n*-heptane decomposition determined from the complete analysis. In fact the liquid phase conversion was found to be numerically equal to C_7 decomposition within limits of ± 5%, an empirical relation which can only be applied to the range of yields and sampling conditions used in the present experiments. Thereafter only liquid samples were taken routinely, but complete sampling was performed occasionally as a check and to obtain additional information about gas product compositions.

Table 1. Range of Variables

Temperature	600° to 750°F.
Pressure	250 lb./sq. in. gauge
Reactor power level	0, 100 kw., or 100 kw. plus fission plate
Dose rate	0, 1,790, or 3,600 rep./min.
Dose	4 to 14 krep.
Moles H_2/mole *n*-C_7	0 to 5
Average residence time	2 to 8 min.

DOSIMETRY

Measurements to characterize the radiation field were made in the beam port before inserting the pressure vessel. Results from plain and cadmium covered gold foil activations combined with rate-meter measurements in G port are summarized in Table 2 (*9, 10*).

Table 2. *G* Port Calibration at 100 kw. with the Port Empty

Thermal neutron flux, n./sq. cm. sec.	$8.6 \times 10^{10} e^{-0.0826L}$ *
Gamma dose rate, rep./min.	$2.1 \times 10^4 e^{-0.167L}$
Cadmium ratio (L = 24 in.)	15

* L is the distance from the core end of the beam port in inches. The reaction vessel was about 20 in. long.

George H. Miley is with the University of Illinois, Urbana, Illinois.

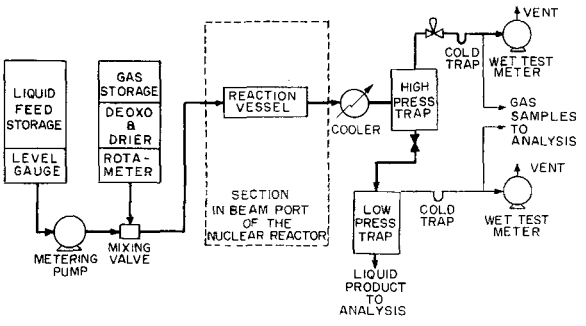

Fig. 1. A simplified flow diagram for the pilot unit.

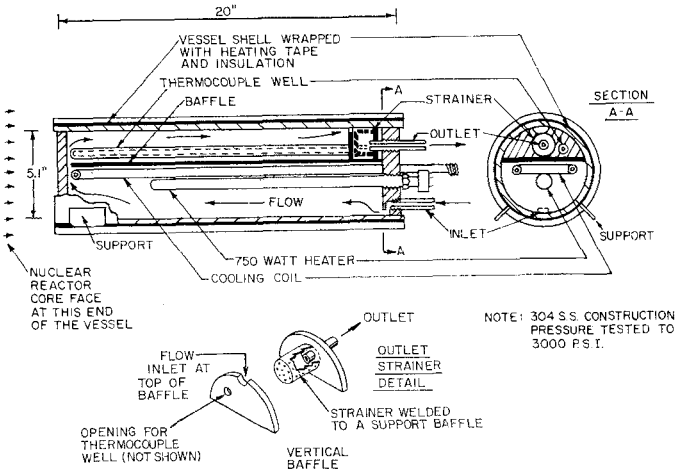

Fig. 2. Irradiation vessel details.

The dose received by a flowing fluid was established by pumping an aerated solution of water saturated with benzene through the vessel and analyzing the product for phenol with a quartz spectrophotometer. Details of the analysis and calibration of this system have been described by Johnson (*12*). Residence times, that is feed rates, were chosen to keep the phenol concentration below 80μ moles/liter where Johnson found a linear relationship; namely

$$C = 2.06\,D \qquad (1)$$

An average flow system dose rate of 1,790 rep./min. was measured for *G* port at 100 kw. Assuming the total dose absorbed by a flowing fluid is proportional to residence time and power level one gets

$$D = \frac{1{,}790 \times 60}{1{,}000}\left[\left(\frac{V}{F}\right)\left(\frac{P}{100}\right)\right] = 1.07\left(\frac{V \times P}{F}\right) \qquad (2)$$

The use of an average residence time V/F implies that the flow pattern in the vessel is independent of flow rate. Runs with feed rates from 6 to 16 liters/hr. checked Equation (2) within several percent. Runs with power levels from 10 to 100 kw. and temperatures from 70° to 190°F. also checked (2) closely. (The phenol yield was found to be independent of temperature in this range, adding to the attractiveness of this dosimetry system.)

Studies in *J* port utilized a fission plate. Comparison of aluminum and magnesium foil threshold measurements with and without the plate in place indicated that the fast neutron flux (> 1 mev.) was roughly doubled by the plate (*13*). Unfortunately the gamma flux was also doubled, giving a total dose rate of 3,600 rep./min., about twice that for *G* port.

RESULTS AND DISCUSSION

Low Yields and Reliability

Short residence times and a temperature range corresponding to the region of incipient thermal cracking were chosen to minimize secondary reactions and to prevent thermal yields from masking radiation effects. These restrictions resulted in conversions of less than 3%. (See Figure 3; as discussed liquid conversion is numerically equal to C_7 decomposition.) The increasing domination of thermal yields at higher temperatures shown in Figure 3 emphasizes the importance of a moderate temperature range.

The use of a flow type of pilot unit to study such low conversions presents many problems. Over-all weight or material balances were consistently better than 99.5% which is believed to be a good check considering possible losses due to pumping, evaporation, etc. However for such low conversions this provides no information about possible coking. Hence the vessel was periodically steamed and cleaned with solvents which were analyzed for polymeric materials. Traces were detected occasionally, but in general the vessel appeared to be very clean. This fact, along with the observation that no products above C_7 were detected from any of the runs, indicates little tendency to coke.

The low yields also raise questions about accuracy. Results are for over seventy runs and consistently good reproducibility was obtained, as illustrated by duplicate runs in Figures 3 and 8 and by the small scatter indicated in all figures. However inaccuracies associated with product analysis, the control of reaction conditions, dosimetry, etc. are compounded in the determination of radiation yields due to differencing conversions from radiation and blank runs. Fortunately, even if an extreme twofold uncertainty is allowed, the results are sufficiently unique to afford some valid conclusions.

G Values and Temperature Effects

Yields from a series of runs from 600° to 750°F. with a H_2/C_7 mole ratio of 0.7 are summarized in Figure 3. The difference in conversion from a radiation run and the paired blank at the same temperature is attributed to radiation. G values shown in Figure 4 were calculated from the relationship

$$G(C_7) = \frac{(Na)\,(CR)}{1{,}000\,D\,(A)\,(MW)} \qquad (3)$$

Absolute conversions were much larger for *J* port fission plate irradiations due to the increased dose rate. However *G* values calculated for *J* and *G* port irradiations are essentially identical, and the values shown in Figure 4 apply to both.

If it is assumed that the *G* value is inversely proportional to the square root of the radiation intensity as indicated by Lucchesi et al. (*7*), lower values would be predicted for *J* port. The constant value obtained could conceivably be attributed to the increased fast neutron flux, implying larger *G* values for fast neutron irradiation. However the results are not conclusive, and further attempts to study fast neutron effects were dropped because clean results could not be obtained. With the available facilities no

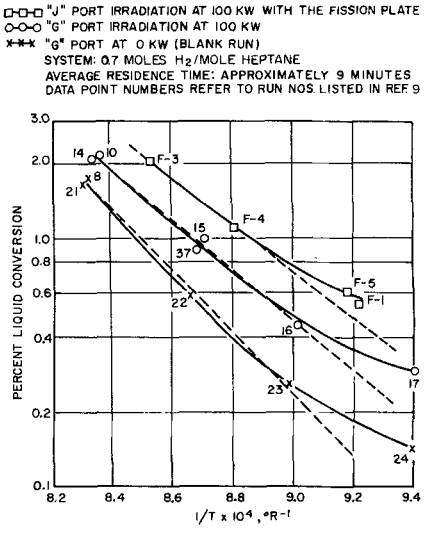

Fig. 3. Liquid conversion vs. temperature.

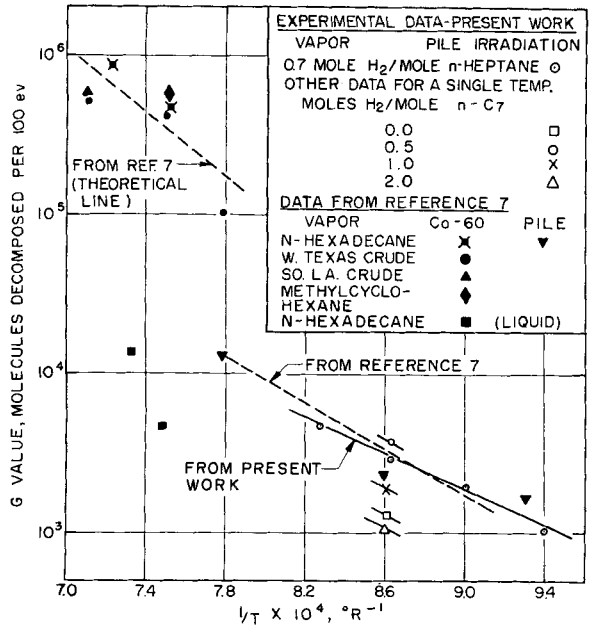

Fig. 4. A comparison of G values obtained with other data from the literature.

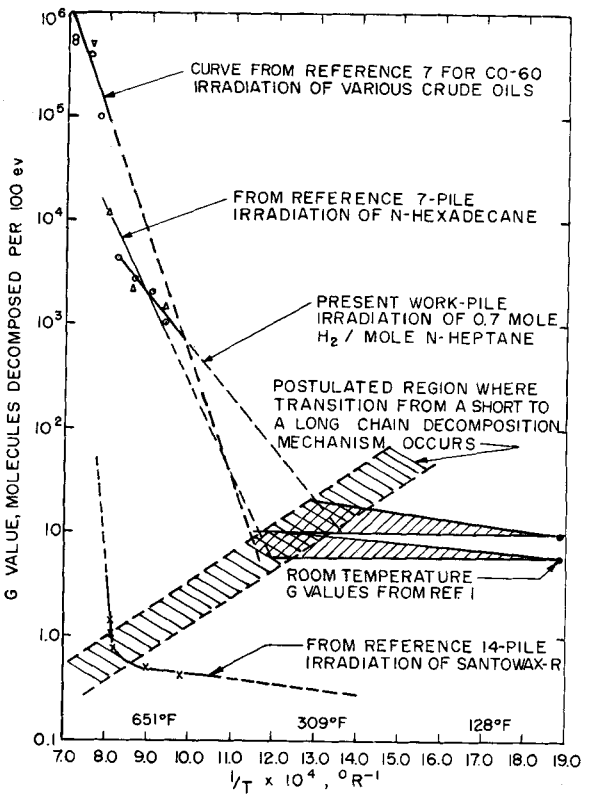

Fig. 5. Illustration of the postulated transition region.

method was found to increase the fast neutron flux without also increasing the gamma flux and thus obscuring neutron effects.

The slope of the *n*-heptane *G* value line in Figure 4 corresponds to an activation energy of about 18 kcal./mole. Both this slope and absolute *G* values agree well with the work of Lucchesi et al. (*7*) shown in Figure 4. Russian workers (*8*) also report *G* values of the order of 10^3 with a 2- to 4-min. irradiation of various gaseous alkanes. Radiation dose rates, pressures, systems, etc. are considerably different for these various experiments; hence *G* value comparisons should be limited to order of magnitude considerations. In particular the close numerical agreement between the present results and the *n*-hexadecane data from reference 7 is probably coincidental. For example the higher pressure used in the present work may have compensated for the lower dose rate.

Lucchesi et al. (*7*) pointed out that even granting a twofold uncertainty the *G* values obtained in their work are significantly higher than those reported for room-temperature measurements. This statement can also be applied to the present results, so that the order of magnitude agreement from separate experiments is particularly significant. Lucchesi et al. have shown that such high *G* values indicate a reaction of moderately long chain length and have proposed a Rice-Herzfeld type of mechanism.

The contrast between high- and low-temperature radiocracking is emphasized in Figure 5. Unfortunately no data has been published for intermediate temperatures, and the available data covers such narrow ranges that extrapolation is risky. The sharply breaking curves shown were selected by comparison with data from the irradiation of santowax-R (terphenyl mixture) at Harwell (*14*). This raises interesting questions. How sharp is the transition to a chain type of reaction? What product distributions arise from intermediate temperature chain reactions? Is there a correlation between molecular weight and the transition temperature? Experiments at intermediate temperatures would answer these and other questions, and it is suggested that this would add substantially to knowledge of radiocracking. In fact there are indications that much work in Russia has concentrated on intermediate temperatures (*8*).

Product Distribution and Mechanisms

Some typical off-gas analyses are listed in Table 3. Despite relatively low temperatures the thermal cracking contribution obtained during radiation runs may have masked small shifts in product distributions (note yields—

Table 3. Typical Gaseous Product Compositions

Run number (*9*)	8	10	61	40	55	F-3	Ref. 20
Reaction conditions							
Gas added	H_2	H_2	—	—	Argon	H_2	—
Moles gas/mole C_7	0.67	0.69	—	—	1.35	0.67	—
Temperature, °F.	742	740	704	701	691	718	1,076
Pressure, lb./sq. in. gauge	250	250	250	250	250	250	15
Radiation	No	Yes	No	Yes	Yes	Fission plate	No
Total conversion, %	1.7	2.2	0.5	0.8	0.8	2.2	6.9
Radiation yield, % of total	—	25	—	38	23	60	—
Off-gas composition (Mole %, H_2 free basis)							
CH_4	14.3	17.1	12.9	10.1	14.2	15.3	18.2
C_2H_4	21.2	19.7	17.2	9.1	18.4	14.5	30.3
C_2H_6	27.3	26.6	25.8	29.8	22.0	27.4	16.2
C_3H_6	19.5	16.3	18.7	22.2	15.6	19.1	16.2
C_3H_8	10.1	10.8	10.7	17.0	13.5	9.2	1.0
C_4H_8	2.4	3.4	4.1	4.1	4.9	5.3	11.1
C_4H_{10}	2.0	1.4	2.2	0.7	4.3	3.1	3.0
$>C_4$	3.3	4.6	8.5	7.1	7.1	6.1	4.0

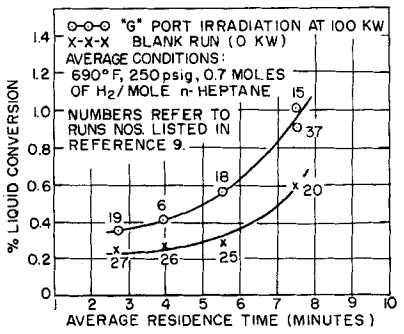

Fig. 6. Liquid conversion vs. average residence time.

Table 3). However no major differences were found between radiation and pure thermal (blank) run product distributions. This is consistent with results reported by others (*7, 8*).

Differences between the present results and other published data for pure thermal cracking (Table 3, column 7) are attributed to dissimilar reaction conditions. This stresses the importance of the small conversions and relatively mild conditions used in the present experiments.

Cracked products through C_6 were observed from the chromatograms of the liquid samples. No products above C_7 were detected and only traces of unsaturated C_7's. As with off-gas compositions a close similarity between radiation and blank-run products was noted.

It appears that both these results and low-temperature data reported in the literature can be represented by a combination of reaction steps suggested by several workers. This is illustrated by Table 4. The general organization and steps 1, 5, 7, 9, and 11 in particular follow the Rice-Herzfeld process proposed by Lucchesi et al. to explain high-temperature results (*7, 15*). Steps have been added to treat hydrogen, and the primary and termination steps have been generalized to include mechanisms suggested by Dewhurst and Krenz to explain room temperature results (*16, 17*).

The high G values obtained at elevated temperatures indicate moderately long chain lengths, and chain reaction products would be expected to completely overshadow those from primary and termination steps. If the chain steps involving hydrogen radicals are neglected, an over-all balance of saturated and unsaturated products is predicted through a combination of steps 5 and 7. This is consistent with the present results, where only products below C_7 were observed and gas analysis indicates an approximate saturate/unsaturate balance. (An exact ratio was not determined, since with the exception of the C_7 fraction an accurate separation of saturate-unsaturates was not made for the liquid samples.) It is interesting that a balance favoring saturates could not be explained by the chain process listed, thus indicating other mechanisms or secondary reactions. Chain steps favoring unsaturates are possible, through a combination of steps 5, 7, and 9, or through steps involving hydrogen production via 6. In fact Topchiev and co-workers (*8*) indicate that somewhat lower temperatures can be used with appropriate dose rate and exposure time to obtain significant yields of unsaturates and molecular hydrogen. This would seem to indicate that it is possible to shift to a chain mechanism based on steps 6, 7, 8, and 10.

The low G values reported for room-temperature irradiation indicate a non-chain process (*1, 2, 7*), and Table 4 is arranged to include such processes as primary and termination steps. A complete product analysis has not been published for heptane, but the following G values reported by Dewhurst (*17*) for the irradiation of *n*-hexane at room temperature are probably indicative of what might be expected:

$$G\ (C_1 \text{ through } C_5) = 2.1$$
$$G\ (C_7 \text{ through } C_{11}) = 1.5$$
$$G\ (C_{12}) = 2.0$$

Reactions of the type indicated by step 11 have been suggested by both Dewhurst and Krenz to explain the yields of higher molecular weight ($> C_6$) products (*16, 17*). Failure to detect products above C_7 in the present work is consistent with the suggested domination of chain-reaction products at high temperature and and the inclusion of step 11 as a termination mechanism.

Dewhurst also noted a significant yield of $C_6^=$ and similar compounds. These and other observations led him to the conclusion that direct unsaturation (step 3) is an important primary step at low temperatures. He also suggests that step 4 is important. The

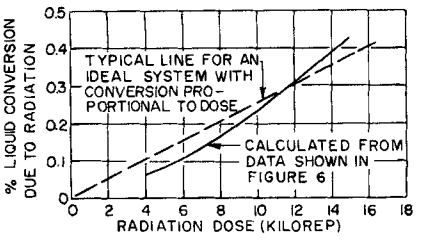

Fig. 7. Radiation conversion (total liquid conversion minus thermal) vs. dose.

absence of significant $C_7^=$ yields in the present work indicates that products from step 3 are insignificant in comparison with chain-reaction products. But both steps 3 and 4 lead directly to stable products, so it is conceivable that while products from these steps are overshadowed, the reactions themselves could still occur with a high frequency relative to 1 or 2 which lead to chain steps. Thus all four steps are retained as possible primary reactions even at high temperatures.

These mechanisms appear to be compatible with the observation by Lucchesi that the hydrogen concentration in off gases decreases with increasing temperature, that is with the change to a chain process (7). Dewhurst (*16*) estimates from his work with hexane that about 30% of the hydrogen yield at low temperatures came from unsaturation and 30% from dimer formation. But based on the absence of significant $C_7^=$ and C_{14} yields in the present work these reactions have been classified as primary and termination reactions, respectively. As previously argued yields from these steps are obscured by chain step products at high temperatures so that a decrease in H_2 concentration (but not necessarily absolute yield) is predicted. This assumes that, as suggested for the present experiments, non-H_2 producing chain steps dominate. As noted earlier it may be possible to shift to a H_2 producing chain reaction under certain conditions. (H_2 yields were not meas-

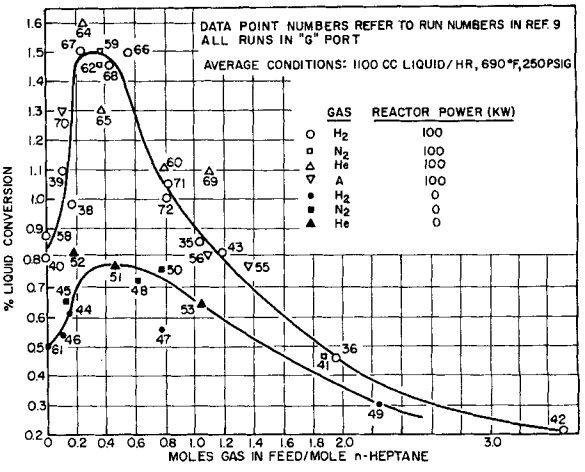

Fig. 8. Liquid conversion vs. molal gas to liquid ratio.

TABLE 4. A COMPOSITE MECHANISM

Primary steps

(1)	$C_7H_{16} \xrightarrow{h\nu} \cdot C_nH_{2n+1} + \cdot C_{7-n}H_{2(7-n)+1}$	C-C rupture, $1 \lesssim n \lesssim 6$
(2)	$C_7H_{16} \xrightarrow{h\nu} \cdot H + \cdot C_7H_{15}$	C-H rupture
(3)	$C_7H_{16} \xrightarrow{h\nu} H_2 + C_7H_{14}$	Direct unsaturation
(4)	$C_7H_{16} \xrightarrow{h\nu} C_nH_{2n} + C_{7-n}H_{2(7-n)+2}$	Molecular rupture, $1 \lesssim n \lesssim 6$
(1A)	$H_2 \xrightarrow{h\nu} \cdot H + \cdot H$	H_2 gas dissociation (if added)

Chain steps

(5)	$\cdot C_nH_{2n+1} + C_7H_{16} \rightarrow C_nH_{2n+2} + \cdot C_7H_{15}$	Saturated product, $1 \lesssim n \lesssim 6$
(6)	$\cdot H + C_7H_{16} \rightarrow H_2 + \cdot C_7H_{15}$	Molecular H_2 product
(7)	$\cdot C_7H_{15} \rightarrow \cdot C_nH_{2n+1} + C_{7-n}H_{2(7-n)}$	Unsaturated product, $1 \lesssim (7-n) \lesssim 6$
(8)	$\cdot C_7H_{15} \rightarrow \cdot H + C_7H_{14}$	Unsaturated C_7
(9)	$\cdot C_nH_{2n+1} \rightarrow \cdot C_kH_{2k+1} + C_{n-k}H_{2(n-k)}$	Unsaturated product, $1 \lesssim (n-k) \lesssim 5$
(10)	$\cdot C_nH_{2n+1} \rightarrow \cdot H + C_nH_{2n}$	Unsaturated product, $1 \lesssim n \lesssim 6$

Termination steps

(11)	$\cdot C_RH_{2R+1} + \cdot C_MH_{2M+1} \rightarrow C_{R+M}H_{2(R+M)+2}$	Saturated product, $2 \lesssim (R+M) \lesssim 14$
(12)	$\cdot H + \cdot C_RH_{2R+1} \rightarrow C_RH_{2R+2}$	Saturated product, $1 \lesssim R \lesssim 7$
(13)	$\cdot H + \cdot H \rightarrow H_2$	Molecular H_2 product
(14)	$\cdot C_RH_{2R+1} + \cdot C_MH_{2M+1} \rightarrow C_RH_{2R+2} + C_MH_{2M}$	Saturated and unsaturated product, $1 \lesssim R, M \lesssim 7$

ured directly in the present work because the H_2 added to the feed made analysis inaccurate.)

Dose and Gas Ratio Effects

Variations in total dose were accomplished at a constant dose rate by changing the feed rate. Results are summarized in Figure 6. The curves appear to extrapolate to a finite conversion at zero residence time. Probably the arbitrary definition of residence time, vessel volume/feed rate, does not represent a true thermal contact time owing to thermal decomposition in the preheater and outlet sections (no quenching provided). This ambiguity is removed however by replotting the data in terms of radiation yield vs. dose as in Figure 7. Thermal effects are subtracted out in determining radiation yields, and the residence time definition cancels out since the residence time-dose correlation was derived with an equivalent flow system.

Radiation yields (Figure 7) extrapolate to zero, but a slight deviation from a linear relationship is noted. A need for additional experiments over a much larger dose range is indicated, since the differences are probably within the limits of experimental accuracy. A dose effect would not be surprising, since primary products might be expected to undergo secondary reactions with long exposures (8, 18). Russian workers have also attributed some differences to the protective radiochemical effect of the decomposition products themselves (8).

Figure 8 summarizes results from runs where the gas (H_2/C_7) ratio in the feed was varied. A constant liquid feed rate was used; hence residence time, total dose, and heptane-partial-pressure all decreased with increasing gas ratio. Normally a continuous reduction in yield would be expected. Instead a pronounced increase in the radiation yield and some increase in the pure thermal yield occurred initially, followed by the expected fall off of both. Possible explanations include energy transfer through the added gas, density effects, and secondary reactions.

It is conceivable that primary energy absorption in hydrogen is more efficient with respect to initiating a chain reaction than absorption in heptane (Table 4). When one discounts recombination, step 1A leads directly to a chain reaction through step 6. In contrast absorption in heptane can be diverted from a chain reaction through steps 3 or 4. However the fact that the substitution of inert gases for hydrogen (Figure 8) did not significantly affect yields raises some doubt about this explanation. Excitation and ionization of these gases could initiate a chain reaction in a manner analogous to hydrogen (19), but it might be expected that the efficiency of energy transfer would be somewhat different for the various gases. Also the increase in yield seems too large in relation to the fractional energy absorption calculated for the added gas at a molal ratio of 0.2 to 0.5.

An alternate explanation which seems somewhat more satisfactory attributes the effect to density or concentration changes alone. Thus in passing from a gas ratio of 0 to 0.5 the system density was greatly reduced and the heptane concentration was cut by a factor of 1½. This might be compared with liquid vs. gas-phase irradiations, where the lower G values obtained for the dense liquid phase are commonly attributed to a cage effect (7). G values have been found to differ by as much as a factor of 100 (note *n*-hexadecane, Figure 4). There is some question as to whether or not caging would occur in the present case with a gas phase at 250 lb./sq. in. gauge. If one assumes it does, a factor of 2 difference for the much smaller density change caused by increasing the gas ratio is not surprising. This explanation is also consistent with the insensitivity of the result to the type of gas added and the observation that some increase in yield also occurred for pure thermal runs.

Off-gas compositions (Table 3) for runs with H_2 and argon added are similar, but there appears to be some tendency for runs without gas added, particularly radiation run number 40, to have a reduced CH_4 and C_2H_4 content along with an increased C_3 content. Differences are very small and may not be within experimental limits of accuracy, but if real, these trends suggest another conceivable explanation for the peaking effect, secondary reactions. The reduced C_2H_4 content in particular suggests ethylene polymerization which is known to have a high G value. However as already discussed there is evidence that coking or long chain polymerization did not normally occur, so that this explanation requires the assumption that it occurred only in the few runs with gas ratio < 0.2. But a mechanism through which polymerization might be inhibited by adding gas to the feed is not clear. Direct reaction with hydrogen must be ruled out, since inert gases produce the same effect. On this basis the secondary reaction hypothesis is not as satisfying as either the energy transfer or the caging explanation.

NOTATION

A = a conversion factor, 5.2 x 10^{13}, ev./g. rep.

C = phenol concentration, μ moles/liter

CR = difference in liquid phase conversion from paired radiation and blank runs, (moles converted by radiation/mole feed) x 100, %

D = total radiation dose received, krep.

$G(X)$ = G value for compound X, number of molecules of X converted per 100 ev. absorbed

L = distance along beam port center line measured from the end nearest the nuclear reactor core, in.

MW = molecular weight, in this case n-heptane, 100.2 g./g.-mole

Na = Avogadro's number, 6.02 x 10^{23} molecules/g.-mole

P = nuclear reactor power level, kw.

V = irradiation vessel volume, in this work 5.3 liters

C_KH_{2K+2} = any one of the series of hydrocarbons designated by letting $K = 1, 2, \ldots$

C_KH_{2K+1} = radical corresponding to the above hydrocarbon

F = flow rate for liquid or gas passing through the irradiation vessel evaluated at the vessel temperature and pressure, liters/hr.

LITERATURE CITED

1. Collinson, E., and A. J. Swallow, *Quart. Rev.*, **9**, No. 4, p. 311 (1955).
2. Tolbert, B. M., and R. M. Lemmon, *Radiation Research*, 3, No. 1, p. 52 (1955).
3. Barr, F. T., H. J. Ogorzaly, and T. A. Reiter, *Petroleum. Ind.*, **2**, No. 4, p. 21 (1959).
4. *British Patent Number 708901* Assigned to the Standard Oil Company of New Jersey (May 12, 1954).
5. Editorial, *Chem. Eng. News*, **38**, No. 14, p. 42 (1960).
6. Editorial, *Nucleonics*, **19**, No. 2, pp. 47-50 (1961).
7. Lucchesi, P. J., B. L. Tarmy, R. B. Long, D. L. Baeder, and J. P. Longwell, *Ind. Eng. Chem.*, **50**, No. 6, p. 879 (1958).
8. Topchiev, A. V., L. S. Polak, N. Y. Chernyak, V. E. Glushnev, I. V. Vereshchinsky, and P. Y. Glazunov, "Large Radiation Sources in Industry, Conference Proceedings," Vol. 2, pp. 131-8, International Atomic Energy Agency, Vienna (1960). Abstract appears in *Nuclear Sci. Abstr.*, **15**, No. 1, p. 35 (1961).
9. Miley, G. H., Ph.D. thesis, Univ. Michigan, Ann Arbor, Michigan (1958); L. C. Card No. Mic 59-3943.
10. *MMPP-110-1*, "Initial Calibration of the Ford Nuclear Reactor," The University of Michigan Memorial Phoenix Project, Ann Arbor, Michigan (June, 1958).
11. "The Ford Nuclear Reactor—Description and Operation," The University of Michigan Memorial Phoenix Project Handbook, Ann Arbor, Michigan (June, 1957).
12. Johnson, T. R., Ph.D. thesis, Univ. Michigan, Ann Arbor, Michigan (1959), (L. C. Card No. Mic 59-4933).
13. Trice, J. B., *Nucleonics*, **16**, No. 7, p. 81 (1958).
14. Editorial, *Nuc. Eng.*, **5**, No. 45, pp. 59-61 (1960).
15. Steacie, E. W. R., "American Chemical Society Monograph Series No. 102," Reinhold, New York (1946).
16. Dewhurst, H. A., *J. Phys. Chem.*, **62**, No. 1, p. 15 (1958).
17. Krenz, F. H., *Nature*, **176**, No. 4493, p. 1113 (1955).
18. Honig, R. E., and C. W. Sheppard, *J. Phys. Chem.*, **50**, No. 2, p. 119 (1946).
19. Lampe, F. W., *Radiation Research*, **10**, No. 6, p. 691 (1959).
20. Appleby, W. G., W. H. Avery, and W. K. Meerbott, *J. Am. Chem. Soc.*, **69**, No. 10, p. 2279 (1947).

Manuscript received August 30, 1960; revision received May 19, 1961; paper accepted May 22, 1961. Paper presented at A.I.Ch.E. Tulsa meeting.

A General Correlation of Vapor-Liquid Equilibria in Hydrocarbon Mixtures

K. C. CHAO and J. D. SEADER

California Research Corporation, Richmond, California

A general correlation of vapor-liquid equilibria in hydrocarbon mixtures is developed. The vaporization equilibrium ratio (K-value) is calculated through a combination of three factors

$$K = \frac{(v^0\gamma)}{(\phi)}$$

The quantity v^0 is a pure liquid component property and is correlated within the framework of Pitzer's modified form of the principle of corresponding states. The quantity γ is calculated from Hildebrand's equation, with regular liquid solutions assumed. The necessary parameters in this equation are specially determined for the very light components. The vapor state quantity ϕ is calculated from Redlich and Kwong's equation of state. The correlation is in the form of a compact set of equations which are especially suitable for application with an electronic digital computer.

The correlation applies to hydrocarbons of various molecular types, including paraffins, olefins, aromatics, and naphthenes. Hydrogen in hydrocarbon mixtures is likewise correlated. The correlation has been tested with a systematic compilation of literature data on mixtures of these components. The over-all average deviation from 2,696 data points is 8.7%.

Previous investigators have used two different approaches in developing correlations of vapor-liquid equilibria in hydrocarbon mixtures: through an equation of state such as the Benedict-Webb-Rubin equation (*2*) to describe the PVT behavior, and through a convergence pressure correlation such as that presented in the National Gasoline Association of America Equilibrium Ratio Data Book (*15*). Both methods are in wide use. Neither of these methods in their present form however satisfies the need for generality. Thus their application is restricted to mixtures containing paraffins and/or olefins. Aromatics and naphthenes are excluded. The same is true of hydrocarbon mixtures containing inert gases such as hydrogen. In view of the growing industrial importance of mixtures containing paraffins, olefins, aromatics, naphthenes, and/or inert gases a more general correlation has been developed to apply to all components in these mixtures.

J. D. Seader is with Rocketdyne, a Division of North American Aviation, Inc., Canoga Park, California.

DESCRIPTION OF CORRELATION

The vaporization equilibrium ratio K_i of component i in a mixture is computed from a combination of three